



Published in final edited form as:

*J Biol Rhythms*. 2013 February ; 28(1): 15–25. doi:10.1177/0748730412468084.

## Aberrant Development of the Suprachiasmatic Nucleus and Circadian Rhythms in Mice Lacking the Homeodomain Protein Six6

Daniel D. Clark<sup>\*,†</sup>, Michael R. Gorman<sup>†,‡</sup>, Megumi Hatori<sup>†,§</sup>, Jason D. Meadows<sup>\*,†</sup>, Satchidananda Panda<sup>†,§</sup>, and Pamela L. Mellon<sup>\*,†,1</sup>

<sup>\*</sup>Department of Reproductive Medicine, University of California, San Diego, La Jolla, CA, USA

<sup>†</sup>Center for Chronobiology, University of California, San Diego, La Jolla, CA, USA

<sup>‡</sup>Department of Psychology, University of California, San Diego, La Jolla, CA, USA

<sup>§</sup>Regulatory Biology Laboratory, Salk Institute for Biological Studies, La Jolla, CA, USA

### Abstract

The suprachiasmatic nucleus (SCN) of the mammalian hypothalamus is the central pacemaker for peripheral and organismal circadian rhythms. The development of this hypothalamic structure depends on genetic programs throughout embryogenesis. We have investigated the role of the homeodomain transcription factor *Six6* in the development of the SCN. We first showed that *Six6* mRNA has circadian regulation in the mouse SCN. We then characterized the behavioral activity patterns of *Six6*-null mice under various photoperiod manipulations and stained their hypothalami using SCN-specific markers. *Six6*-null mice display abnormal patterns of circadian behavior indicative of SCN abnormalities. The ability of light exposure to reset rhythms correlates with the presence or absence of optic nerves, but all *Six6*-null mice show irregular rhythms. In contrast, wild-type mice with crushed optic nerves maintain regular rhythms regardless of light exposure. Using immunohistochemistry for arginine vasopressin (AVP), vasoactive intestinal polypeptide (VIP), and  $\beta$ -galactosidase, we demonstrated the lack of these SCN markers in all *Six6*-null mice regardless of the presence of optic nerve or partial circadian rhythms. Therefore, *Six6* is required for the normal development of the SCN, and the *Six6*-null mouse can mount independent, although irregular, circadian rhythms despite the apparent absence of a histochemically defined SCN.

### Keywords

homeodomain protein; suprachiasmatic nucleus; circadian rhythm; *Six6*; development; optic nerve

---

The suprachiasmatic nucleus (SCN) of the mammalian hypothalamus is a central pacemaker of circadian rhythms. Physical ablation of this nucleus in rodents leads to behavioral and

---

© 2013 The Author(s)

<sup>1</sup>To whom all correspondence should be addressed: Pamela L. Mellon, Department of Reproductive Medicine, 3A14, Leichtag Biomedical Sciences Building, University of California, San Diego, School of Medicine, 9500 Gilman Drive, La Jolla, CA 92093-0674, USA; pmellon@ucsd.edu.

### CONFLICT OF INTEREST STATEMENT

The authors have no potential conflicts of interest with respect to the research, authorship, and/or publication of this article.

### NOTE

Supplementary online material is available on the journal's website at <http://jbr.sagepub.com/supplemental>.

physiological arrhythmicity (Stephan and Zucker, 1972) and impaired fertility (Wiegand and Terasawa, 1982). Light input from photosensitive ganglion cells in the eye, via a retino-hypothalamic tract in the optic nerve, entrains the SCN's approximately 24-h activity patterns to advance or delay the phase of rhythm such that the physiology of the animal is appropriately timed to its environmental context (Panda et al., 2002).

*Six6*, a murine homeobox gene orthologous to *Drosophila optix* (Jean et al., 1999), has been shown to play important roles in the developing eye, brain, and pituitary. It is expressed as early as 8 days post-conception in the mouse. Throughout development, it is expressed in the hypothalamus, the pituitary, and the olfactory placode and is later expressed in the optic vesicle, the optic stalk, and the retina (Jean et al., 1999). In adult, it remains expressed in the hypothalamus, as well as cells of the eye and pituitary (Conte et al., 2005). Deletion of the mouse *Six6* gene leads to defects in precursor cell proliferation in the retina and pituitary (Li et al., 2002).

*Six3* is a close homolog of *Six6*, and the two share partially overlapping expression patterns (Jean et al., 1999). *Six3* and *Six6* were among several transcription factors recently identified as being expressed early in development and strongly in the postnatal SCN (VanDunk et al., 2011). Neuronal deletion of *Six3* was accomplished by breeding a LoxP-flanked *Six3* allele-bearing mouse line (Liu et al., 2006) with a mouse line expressing Cre recombinase under the control of a neuron-specific enhancer from the *Nestin* gene (Tronche et al., 1999). Mice with complete neuronal deletion of *Six3* lacked a number of markers for the SCN. This was in contrast to the presence of normal SCN in mice lacking functional *RORα* (Hamilton et al., 1996), a gene also expressed strongly in the SCN and early in development. However, the role of *Six3* or *Six6* in the postnatal mouse, either behaviorally or anatomically, has not yet been investigated.

Recently, *Six6* was shown to play a critical role in reproduction (Larder et al., 2011). Gonadotropin-releasing hormone- (GnRH-) secreting neurons in the hypothalamus control the pituitary gonadotrope cells that, in turn, control reproduction. In a screen to identify genes important for GnRH neuron function, *Six6* expression was 100-fold greater in a cell model of mature (GT1-7 line) versus immature (GN11 line) GnRH neurons. Female mice lacking *Six6* showed a profound infertility phenotype; only 1 *Six6*-null female out of an experimental cohort of 8 was able to deliver a single litter over 3 months. Also, both male and female *Six6*-null mice had significantly reduced numbers of GnRH neurons (90% reduced). In addition, an altered pattern of tyrosine hydroxylase expression in the hypothalamus suggested a more general role for *Six6* in the development of the hypothalamus.

Given the developmental and spatial expression pattern of *Six6* and the role of its homolog *Six3* in the formation of the SCN, interesting questions remained concerning the role of *Six6* in the brain. Does *Six6* expression follow a circadian rhythm, and is *Six6* a target or component of the molecular circadian clock? Do mice lacking *Six6* also lack a normal SCN, as observed in the neuron-specific *Six3*-null mice, or is the SCN of *Six6*-null mice intact, as observed for the *RORα*-null mice?

While the developmental and spatial expression pattern of *Six6* has been reported in the mouse (VanDunk et al., 2011), its expression in the SCN over circadian time is not known. We demonstrated a circadian temporal expression pattern of *Six6* in the adult hypothalamus and altered circadian behavioral phenotypes of *Six6*-null mice. The mouse SCN is characterized by a vasoactive intestinal polypeptide- (VIP-) positive core region at its ventral base and an arginine vasopressin- (AVP-) positive shell region surrounding the core dorsally, and staining for these 2 proteins has been used extensively to characterize the SCN

(Leak and Moore, 2001). The SCN of the *Six6*-null mouse was characterized using immunohistochemical staining for these 2 SCN markers, as well as morphological analysis, indicating that the SCN fails to fully develop in the *Six6*-null mouse.

## MATERIALS AND METHODS

### Animals and Housing

*Six6*-null mice were obtained from Dr. Xue Li (Children's Hospital of Boston, Harvard Medical School, Boston, MA) and were maintained in accordance with protocols approved by the University of California, San Diego, and the Salk Institute for Biological Studies Institutional Animal Care and Use Committees. Animals were housed under 12 h:12 h light:dark lighting conditions, except as noted below, and were given ad libitum access to food and water. Our colony was maintained on a mixed 129/Sv (original) and C57BL/6 (3-generation backcross) background strain.

### Quantitative Reverse-Transcriptase Polymerase Chain Reaction

Male mice heterozygous for the *Six6* deletion allele were euthanized via overdose of inhaled isoflurane anesthetic at zeitgeber time 20 (ZT20), 4 h prior to lights on (in the dark,  $n = 4$ ) and at ZT8, 4 h prior to lights off ( $n = 4$ ). Hypothalami were dissected and transferred to Trizol reagent (Life Technologies, Carlsbad, CA). RNA was extracted according to the manufacturer's instructions. cDNA was prepared using a SuperScript III first-strand cDNA synthesis kit (Life Technologies). Quantitative polymerase chain reaction (PCR) was performed using a BioRad (Hercules, CA) iQ5 system and B-R-SYBR Green (Quanta Biosciences, Gaithersburg, MD). Gene-specific PCR primers (Suppl. Table S1) were used to determine the expression levels of mouse *Six3*, *Six6*, *Bmal* (*Arntl*), and *Per2*, along with the control genes *Gapdh*, *H2afz*, and *Ppia*. Known quantities of reference DNA plasmids each containing a gene of interest were used to prepare standard curves, against which the hypothalamic expression levels were measured. Expression of each gene of interest was normalized to the geometric average of the expression of the three control genes at each time point (Vandesompele et al., 2002).

### Photoperiod Manipulations

*Six6*-null mice ( $n = 6$ ) and wild-type (WT) littermate controls ( $n = 6$ ) were raised in a 12 h:12 h light:dark photoperiod until 2 to 4 months of age. Mice were then introduced into cages containing running wheels equipped with magnets and monitored using magnetic switches. All cages were contained within a light-tight cabinet with programmable fluorescent lighting. The previous photoperiod was maintained, and the mice were given 7 days to acclimate to the new environment. Wheel turns were recorded for each mouse in 6-min bins and analyzed offline using the Clocklab (Actimetrics, Wilmette, IL) suite of Matlab (Mathworks, Natick, MA) plugins. Actograms were plotted using the above software, Microsoft Excel, and an online plotting program produced by Roberto Refinetti (<http://www.circadian.org/actogram.html>, accessed 2011). Four different photoperiod manipulations were performed: (1) a 12 h:12 h light:dark schedule, (2) complete darkness, (3) a 1 h:11 h L:D skeleton photoperiod, and (4) a 6 h:6 h:6 h:6 h L:D:L:D, bifurcated light schedule. The final schedule included illumination with dim, narrowband green light ( $555 \pm 23$  nm;  $<0.1$  lux) throughout all scotophases as shown previously to facilitate bifurcated entrainment in rodents (Gorman et al., 2003).

### Hypothalamic Immunohistochemical and Cytological Staining

Mice were cardiac perfused with a phosphate-buffered saline (PBS) solution followed by a 4% formalin solution of PBS. Brains were dissected from the skull and postfixed for 16 h in

a 4% formalin PBS solution. Brains were then transferred to a 50% sucrose solution of PBS for 12 h and then embedded in O.C.T. compound (Tissue-Tek; Sakura Finetek USA, Torrance, CA) and frozen at  $-80^{\circ}\text{C}$ . Brains were sectioned at  $20\ \mu\text{m}$  and thaw mounted onto PermaFrost plus glass slides. Brain sections were stained using 1 of 3 primary antibodies: polyclonal rabbit anti-VIP (ImmunoStar, Hudson, WI), rabbit antivasopressin (ImmunoStar), or rabbit antityrosine hydroxylase (Pel-Freez, Rogers, AR). For the  $\beta$ -galactosidase staining, brains were dissected, placed on dry ice, and stored at  $-80^{\circ}\text{C}$  until being sectioned at  $20\ \mu\text{m}$ . These sections were then stained using polyclonal chicken anti- $\beta$ -galactosidase (Abcam, Cambridge, UK). Slides were then processed and stained with a peroxidase substrate chromogen kit (Vector VIP; Vector Labs, Burlingame, CA) according to the manufacturer's recommendations. Following further rinses and an alcohol dehydration series, slides were air dried and mounted with cover-slips.

Cresyl violet Nissl staining was performed on  $20\text{-}\mu\text{m}$ -thick cryostat brain sections. Slides were rinsed and then exposed to a 0.5% cresyl violet solution for 30 min and then processed as above for final coverslipping.

### Optic Nerve Crush Surgery

The circadian wheel-running activity of 8-week-old male C57BL/6J mice was collected and analyzed as described (Siepkka and Takahashi, 2005). After 10 days of baseline activity under a standard 12 h:12 h light:dark photoperiod, mice were anesthetized with ketamine and xylazine. The optic nerves of both eyes were exposed intraorbitally. Using a No. 5 forceps, the optic nerve, approximately 1 mm distal to the optic disc, was crushed for several seconds (for control mice, optic nerves were exposed but not crushed). After recovery, the mice were returned to the wheel-running cages, and their activity was monitored. Subsequent photoperiod manipulations included LD, DD (constant darkness), and LL (constant light).

## RESULTS

### Diurnal Expression Pattern of *Six6* mRNA

Quantitative reverse-transcription PCR was used to measure the expression levels of *Six3* and *Six6* at 2 zeitgeber time points. The 2 time points chosen are near the expected times of maximal and minimal expression of the known clock genes *Bmal1* and *Per2*. These time points are also near the times of maximal and minimal expression of *Six3* (VanDunk et al., 2011). As expected, at ZT8, the hypothalamic expression of *Bmal1* is significantly lower and expression of *Per2* is significantly higher than their expression at ZT20 (Fig. 1). Expression of *Six3* mRNA is significantly lower at ZT20 than at ZT8, and this finding is consistent with a previous report (VanDunk et al., 2011). *Six6* mRNA expression was significantly lower at ZT20 than at ZT8, indicating that *Six6* expression appears to also be diurnally regulated (Fig. 1).

### Abnormal Photoperiod Entrainment of the *Six6*-Null Mouse

WT mice entrained normally to the 12 h:12 h photoperiod, as assessed by their wheel-running activity (Fig. 2). WT mice showed robust wheel running during the dark portion of the photoperiod, almost complete absence of activity during the light portion of the photoperiod, and evidence of negative masking at the light/dark transitions. For reference, Supplemental Figure S1 includes the activity profile for the 2 WT and 6 *Six6*-null mice for the entire period of observation. Because the *Six6*-null mice showed a wide variety of activity patterns, qualitative and descriptive analyses of the behavioral rhythms were used in addition to quantitative analyses. Two of the 6 *Six6*-null mice did not appear to have any differences in wheel-running behavior between light and dark portions of the photoperiod

(Six6 KO C; Fig. 2). Other *Six6*-null mice showed greater activity during the dark portion of the photoperiod than the light portion, but the activity bouts did not show the characteristic sharp onset and gradual offset of activity during the dark; rather, there appeared to be 2 separate bouts of activity following lights-off and prior to lights-on (Six6 KO A). Finally, 2 of the *Six6*-null mice showed nearly normal entrainment to the L:D photoperiod (Six6 KO B).

### Variable Optic Nerve Phenotype in *Six6*-Null Mice

The presence of the optic nerve is variable in *Six6*-null mice (Li et al., 2002). WT and null animals were sacrificed and dissected. As the brain was dissected, care was taken to note the size and presence of each optic nerve. All WT mice had normal optic nerves, but *Six6*-null mice had 1 of 3 optic nerve phenotypes (Fig. 2). Half of the *Six6*-null mice studied ( $n = 7/14$ ) had no optic nerve or threadlike, severely atrophied, or poorly developed optic nerves, with no visible optic chiasm (e.g., Six6 KO C). Interestingly, the eyes of these *Six6*-null mice appeared relatively normal, with no obvious atrophy or lid closure. A second phenotype ( $n = 5/14$ ) of *Six6*-null mice was characterized by the presence of either the right or the left optic nerve, with the other completely missing (e.g., Six6 KO B). A third *Six6*-null phenotype ( $n = 2/14$ ) was characterized by the presence of both optic nerves but a lack of chiasm (e.g., Six6 KO A). In these mice, the optic nerves appear to project to the thalamus without forming a chiasm. It is unclear whether all or some of the retinohypothalamic tract is missing in these mice.

### Abnormal Free-Running Activity of the *Six6*-Null Mouse

Following photoperiod entrainment, WT and *Six6*-null mice were released into constant darkness. With no environmental cues indicative of day length, WT mice ( $n = 6$ ) retained robustly rhythmic activity patterns with a period of  $\tau = 23.7 \pm 0.16$  h. However, *Six6*-null mice displayed a range of activity patterns in constant darkness (Fig. 3). *Six6*-null mice with single or double intact optic nerves showed a range of free-running activity patterns, with some showing strong circadian periodicity ( $n = 3$ ,  $\tau = 24.40 \pm 0.50$ , and 1 showing weak circadian periodicity (multiple weak  $\chi^2$  periodogram peaks; 6 KO B from Fig. 3). Neither of the 2 *Six6*-null mice without optic nerves had strong circadian rhythms, but 1 had strong ultradian periodicity (fast Fourier transform [FFT] peak = 6.40 h, relative power = 0.12; Fig. 3), while the other had weak ultradian periodicity (FFT peak = 7.00 h, relative power = 0.04).

### Abnormal Skeleton Photoperiod Activity of the *Six6*-Null Mouse

Given the abnormal and variable activity patterns of the *Six6*-null mice during standard 12 h:12 h photoperiods and under constant darkness, we subjected WT and *Six6*-null mice to 2 additional alternative photoperiods. Rodents are capable of entraining to brief, 1-h pulses of light given every 12 h (Pittendrigh and Daan, 1976). Robust activity is typically consolidated in 1 of the 2 long dark intervals between light pulses (subjective night) with inactivity in the opposite dark phase (subjective day). Wild-type mice behaved as expected, with all 6 wild-type mice displaying unambiguous subjective night and subjective day activity patterns (Fig. 4). There was no clear demarcation of subjective day and night for 3 of the 4 *Six6*-null mice with at least 1 optic nerve; their activity was distributed equally between the light pulses. The *Six6*-null mice with no optic nerves continued to exhibit only an unentrained ultradian pattern of activity.

We then subjected WT and *Six6*-null mice to a bifurcated, 6 h:6 h:6 h:6 h, L:D:L:D photoperiod to investigate whether the behavioral activity patterns would be different with an increased frequency of dark onset. In a bifurcated photoperiod with 4 light/dark

transitions per 24 h, *Six6*-null mice with intact optic nerves showed strong activity during the dark portion of the photoperiod, as did WT mice (Fig. 4).

### ***Six6*-Null Mouse SCN Phenotype**

WT and the 3 types of *Six6*-null mouse hypothalami were sectioned and stained for the SCN markers AVP and VIP as described in the Materials and Methods section. Given that the range of circadian phenotypes varied along with optic nerve phenotypes, we hypothesized that the SCN of *Six6*-null mice would similarly vary. All WT mice had discrete, bilateral SCN morphologically identifiable through the dense ventral hypothalamic region of small cell bodies characteristic of the SCN, prominent following immunohistochemical or cytological staining (Fig. 5; also, see Supplemental Online Material for a full, section-matched, rostral-caudal staining series for WT and *Six6*-null mice). However, no *Six6*-null mouse, regardless of optic nerve phenotype, showed evidence for a histochemically (AVP and VIP) defined SCN. Moreover, general cytological staining (cresyl violet Nissl) did not reveal morphologically distinct SCN nuclei in any *Six6*-null mice (Fig. 6). As described previously for the conditional *Six3*-null mice, other hypothalamic nuclei with AVP-positive neurons (e.g., the supraoptic and paraventricular nuclei; VanDunk et al., 2011) were present in *Six6*-null mice (Suppl. Fig. S2). Interestingly, the AVP-positive supraoptic nuclei are present in *Six6*-null mice lacking optic nerves. The inability to morphologically or histochemically identify SCN in any of the *Six6*-null mice studied, regardless of optic nerve phenotype, indicates that *Six6* plays a role in the development of the SCN independent of the defects seen in the optic nerve. Thus, *Six6* itself is required for the full development of the SCN.

In addition, we performed immunohistochemistry for the marker  $\beta$ -galactosidase. The *Six6*-null allele contains an IRES-LacZ reporter gene in place of the 6 domain and the homeodomain portions of *Six6* (Li et al., 2002) such that  $\beta$ -galactosidase staining indicates the pattern of *Six6* gene expression in the SCN. Mice heterozygous for the null allele (*Six6* +/-) showed strong  $\beta$ -galactosidase staining focused within the SCN, and *Six6*-null mice (*Six6* -/-) showed a scattered pattern of  $\beta$ -galactosidase staining but an absence of the focused pattern found in the normal SCN (Suppl. Fig. S3). These results indicate that the *Six6* promoter is active in some neurons despite the apparent lack of normal SCN morphology.

### **Requirement for the Optic Nerves for Photoperiod Entrainment but Not Circadian Rhythmicity**

The optic nerves relay light information to multiple brain targets. These targets include the SCN, via the retinohypothalamic tract portion of the optic nerves, where light information is capable of resetting (entraining) the circadian clock to match external conditions (photoperiod). In genetically WT adult mice, we confirmed that the inputs from the optic nerve were necessary for the maintenance of circadian rhythmicity of wheel-running behavior. WT mice were given either a sham surgery or an optic nerve crush surgery as described in the Materials and Methods section, and wheel-running activity was monitored under various photoperiods (Fig. 7). The sham surgery resulted in normal entrainment behavior under LD (standard photoperiod), DD (constant darkness), and LL (constant light). A 12-h shift in the LD photoperiod also resulted in normal, robust re-entrainment to the new photoperiod within 4 or 5 days. The optic crush surgery resulted in a total loss of entrainment. However, circadian rhythmicity remained intact, with a strong, stable onset of wheel-running activity throughout the postsurgical activity monitoring. As expected, the lack of optic nerves in the WT adult mouse had no effect on circadian rhythmicity, although entrainment was lost.

## DISCUSSION

The developmental origins of the mouse SCN have been examined using BrdU labeling (Kabrita and Davis, 2008) as well as transcription factor expression profiling (VanDunk et al., 2011). Beginning around embryonic day 12 (Kabrita and Davis, 2008), the first cells of the SCN undergo terminal differentiation in the core region that will eventually become VIP positive (Shimogori et al., 2010). On embryonic days 13.5 to 14, the cells of the shell terminally differentiate. This developmental process likely shares many of the general principles of neurodevelopment, with transcription factors, signaling events, and environmental cues playing a role.

Prior to the birth of the earliest SCN cells, the retinal ganglion cells send their axons (embryonic day 13) to their thalamic targets (Hinds and Hinds, 1974; Lund and Blunt, 1976). However, the retinohypothalamic tract does not innervate the rat SCN until after birth (Mason et al., 1977; Stanfield and Cowan, 1976) and innervates the mouse SCN postnatally (McNeill et al., 2011), after the SCN has formed and begun expression of the markers VIP and AVP. Since the formation of the optic nerves precedes the formation of the SCN and lies in such close proximity to it, the SCN may, in some part, rely on signaling from the optic nerves for its formation. However, the variability of the *Six6*-null mouse optic nerve phenotype indicates that the optic nerve may not be sufficient to initiate formation of the SCN.

In rodents blinded via orbital enucleation, the morphology of the SCN is altered. In rats enucleated (bilaterally or unilaterally) at 4 weeks of age, the optic chiasm becomes thinner, SCN is displaced rostrally, and the number of cells in the typical location of the SCN is decreased (Nagai et al., 1992). However, the overall number of cells in the SCN was not affected by enucleation. The enucleation experiments were performed in rats at 4 weeks of age and thus reflect changes to the SCN after its initial development.

Previous work on transgenic and mutant mouse lines has explored the retinohypothalamic tract and its role in SCN development and physiology. Early work on the *eyeless* mouse (strain ZRDCT-AN [Chase and Chase, 1941] later confirmed to possess a single nucleotide polymorphism removing an alternate start codon of the *Rx/rax* gene [Tucker et al., 2001]) revealed hypothalamic and optic tract deficiencies (Silver, 1977; Laemle et al., 2002) in these mice. The SCN of the *eyeless* mouse strain is variably atypical, with 70% showing normal SCN morphology and cell densities and the remaining mice showing laterally asymmetric deficiencies in SCN size and cell number (Silver, 1977). Seventy-five percent of anophthalmic mice studied (Laemle and Ottenweller, 1998) showed stable circadian activity rhythms, 10% showed unstable rhythms, and 15% were behaviorally arrhythmic. In contrast to the *Six*-null mice reported here, the anophthalmic arrhythmic mice did not show any predominant ultradian periodicity. Whether these SCN and behavioral phenotypes are due to developmental or genetic variability is unknown, but this phenotypic variability is shared with the *Six* null mice.

The SCN phenotype in *Six6*-null mice is not likely due to a lack of light input via the retinohypothalamic tract to the SCN. Mice lacking rod and cone cells and the *melanopsin* (*Opn4*) gene display robust circadian rhythmicity, although this rhythmicity is not entrainable by light (Panda et al., 2003). From in utero through adulthood, these mice have no functional light input to the SCN, suggesting that this input is not necessary for SCN development and function. The optic nerves and optic chiasm in those mice, however, are intact.

The activity patterns of the *Six6*-null mice share some similarity to the activity patterns of mice in which the genes for VIP and peptide histidine leucine (PHI) were deleted (Colwell

et al., 2003). These 2 SCN signaling molecules are capable of phase shifting the circadian clock when administered exogenously. Inactivation of these 2 genes led to mice with altered or arrhythmic behavior in constant darkness, similar to that seen in *Six6*-null mice. In addition, *VIP/PHI*-null mice under a 1 h:11 h skeleton photoperiod did not display consolidated subjective days and nights; this is also similar to the activity patterns observed for the *Six6*-null mice. Another similarity that the *Six6*-null mice share with *VIP/PHI*-null mice is an increased number of activity bouts, with increased activity during subjective day in constant darkness. In constant darkness, the ultradian activity patterns of the *Six6*-null mice lacking optic nerves are qualitatively similar to *VIP/PHI*-null mice.

Whether or not the optic nerves of *Six6*-null mice form properly during development and then atrophy, or do not form at all, remain interesting questions. While further studies are needed to explore the relationship between optic nerve formation and SCN development, using morphological and histochemical approaches, we were not able to identify SCN in any *Six6*-null mice. This finding likely rules out the obvious hypothesis that the SCN phenotype of the *Six6*-null mice is secondary to the optic nerve phenotype.

However, *Six6*-null mice with partially spared optic nerves show some behavioral circadian rhythmicity while lacking apparent SCN, including the absence of AVP and VIP staining and morphological clustering of cells. While the role *Six6* plays in the molecular clock—if any—is currently unknown, it is possible that *Six6*-null mice have a functioning cellular circadian clock in the apparent absence of normal SCN. If the molecular clock is functional in other brain regions (e.g., SCN neurons not located in a cytologically distinct hypothalamic nucleus or present only in small numbers) or peripheral organs (e.g., the liver), this may explain some of the residual behavioral rhythmicity observed in the *Six6*-null mice (Fig. 3, Supp. Fig. S1). The *Six6*-null mouse therefore serves as an excellent model in which this possibility may be explored.

In the present study, SCN morphology and expression of 2 SCN neuropeptides was characterized in WT and *Six6*-null mice. Other important neuropeptides are present in the SCN and may retain WT levels of expression in the absence of *Six6*, including GRP, PRK2, and Nms, and immunohistochemical characterization of these peptides in *Six6*-null mice is one future direction for this line of research. Another future approach to fully characterize the SCN—or lack thereof—in *Six6*-null mice would be to measure the embryonic and adult expression of genes such as *Lhx1*, *Six3*, *Rora*, *Gad67*, and *Calbindin*.

## Supplementary Material

Refer to Web version on PubMed Central for supplementary material.

## Acknowledgments

The authors thank Dr. Xue Li (Children's Hospital of Boston, Harvard Medical School, Boston, MA) for providing *Six6*-null mice, Sunamita Leming for technical assistance, and Rachel Larder for helpful discussions. This work was supported by supported by NIH grants R01 DK044838, R01 HD072754, and R01 HD020377 (to P.L.M.), NIH grant R01 HD036460 (to M.R.G.), NIH grant R01 EY016807 (to S.P.), Japan Society for the Promotion of Science (JSPS) fellowship (to M.H.), and by NICHD/NIH through a cooperative agreement (U54 HD012303) as part of the Specialized Cooperative Centers Program in Reproduction and Infertility Research (P.L.M.). P.L.M. was supported in part by P30 DK063491, P30 CA023100, and P42 ES010337. D.D.C. was supported in part by T32 GM008666 and T32 DK007541 and was a student in the University of California, San Diego, Biological Sciences Graduate Program.

## REFERENCES

- Chase HB, Chase EB. Studies on an anophthalmic strain of mice I. Embryology of the eye region. *J Morphology*. 1941; 68:279–301.
- Colwell CS, Michel S, Itri J, Rodriguez W, Tam J, Lelievre V, Hu Z, Liu X, Waschek JA. Disrupted circadian rhythms in VIP- and PHI-deficient mice. *Am J Physiol Regul Integr Comp Physiol*. 2003; 285:R939–949. [PubMed: 12855416]
- Conte I, Morcillo J, Bovolenta P. Comparative analysis of Six 3 and Six 6 distribution in the developing and adult mouse brain. *Dev Dyn*. 2005; 234:718–725. [PubMed: 15973738]
- Gorman MR, Elliott JA, Evans JA. Plasticity of hamster circadian entrainment patterns depends on light intensity. *Chronobiol Int*. 2003; 20:233–248. [PubMed: 12723883]
- Hamilton BA, Frankel WN, Kerrebrock AW, Hawkins TL, FitzHugh W, Kusumi K, Russell LB, Mueller KL, van Berkel V, Birren BW, et al. Disruption of the nuclear hormone receptor RORalpha in staggerer mice. *Nature*. 1996; 379:736–739. [PubMed: 8602221]
- Hinds JW, Hinds PL. Early ganglion cell differentiation in the mouse retina: an electron microscopic analysis utilizing serial sections. *Dev Biol*. 1974; 37:381–416. [PubMed: 4826283]
- Jean D, Bernier G, Gruss P. Six6 (Optx2) is a novel murine Six3-related homeobox gene that demarcates the presumptive pituitary/hypothalamic axis and the ventral optic stalk. *Mech Dev*. 1999; 84:31–40. [PubMed: 10473118]
- Kabrita CS, Davis FC. Development of the mouse suprachiasmatic nucleus: determination of time of cell origin and spatial arrangements within the nucleus. *Brain Res*. 2008; 1195:20–27. [PubMed: 18201688]
- Laemle LK, Hori N, Strominger NL, Tan Y, Carpenter DO. Physiological and anatomical properties of the suprachiasmatic nucleus of an anophthalmic mouse. *Brain Res*. 2002; 953:73–81. [PubMed: 12384240]
- Laemle LK, Ottenweller JE. Daily patterns of running wheel activity in male anophthalmic mice. *Physiol Behav*. 1998; 64:165–171. [PubMed: 9662081]
- Larder R, Clark DD, Miller NL, Mellon PL. Hypothalamic dysregulation and infertility in mice lacking the homeodomain protein Six6. *J Neurosci*. 2011; 31:426–438. [PubMed: 21228153]
- Leak RK, Moore RY. Topographic organization of suprachiasmatic nucleus projection neurons. *J Comp Neurol*. 2001; 433:312–334. [PubMed: 11298358]
- Li X, Perissi V, Liu F, Rose DW, Rosenfeld MG. Tissue-specific regulation of retinal and pituitary precursor cell proliferation. *Science*. 2002; 297:1180–1183. [PubMed: 12130660]
- Liu W, Lagutin OV, Mende M, Streit A, Oliver G. Six3 activation of Pax6 expression is essential for mammalian lens induction and specification. *EMBO J*. 2006; 25:5383–5395. [PubMed: 17066077]
- Lund RD, Blunt AH. Prenatal development of central optic pathways in albino rats. *J Comp Neurol*. 1976; 165:247–264. [PubMed: 54370]
- Mason CA, Sparrow N, Lincoln DW. Structural features of the retinohypothalamic projection in the rat during normal development. *Brain Res*. 1977; 132:141–148. [PubMed: 890472]
- McNeill DS, Sheely CJ, Ecker JL, Badea TC, Morhardt D, Guido W, Hattar S. Development of melanopsin-based irradiance detecting circuitry. *Neural Dev*. 2011; 6:8. [PubMed: 21418557]
- Nagai N, Nagai K, Nakagawa H. Effect of orbital enucleation on glucose homeostasis and morphology of the suprachiasmatic nucleus. *Brain Res*. 1992; 589:243–252. [PubMed: 1393592]
- Panda S, Provencio I, Tu DC, Pires SS, Rollag MD, Castrucci AM, Pletcher MT, Sato TK, Wiltshire T, Andahazy M, et al. Melanopsin is required for non-image-forming photic responses in blind mice. *Science*. 2003; 301:525–527. [PubMed: 12829787]
- Panda S, Sato TK, Castrucci AM, Rollag MD, DeGrip WJ, Hogenesch JB, Provencio I, Kay SA. Melanopsin (Opn4) requirement for normal light-induced circadian phase shifting. *Science*. 2002; 298:2213–2216. [PubMed: 12481141]
- Pittendrigh CS, Daan S. A functional analysis of circadian pacemakers in nocturnal rodents IV: entrainment: pacemaker as clock. *J Comp Physiol A*. 1976; 106:291–331.
- Shimogori T, Lee DA, Miranda-Angulo A, Yang Y, Wang H, Jiang L, Yoshida AC, Kataoka A, Mashiko H, Avetisyan M, et al. A genomic atlas of mouse hypothalamic development. *Nat Neurosci*. 2010; 13:767–775. [PubMed: 20436479]

- Siepkha SM, Takahashi JS. Methods to record circadian rhythm wheel running activity in mice. *Methods Enzymol.* 2005; 393:230–239. [PubMed: 15817291]
- Silver J. Abnormal development of the suprachiasmatic nuclei of the hypothalamus in a strain of genetically anophthalmic mice. *J Comp Neurol.* 1977; 176:589–606. [PubMed: 925203]
- Stanfield B, Cowan WM. Evidence for a change in the retino-hypothalamic projection in the rat following early removal of one eye. *Brain Res.* 1976; 104:129–136. [PubMed: 1247898]
- Stephan FK, Zucker I. Circadian rhythms in drinking behavior and locomotor activity of rats are eliminated by hypothalamic lesions. *Proc Natl Acad Sci U S A.* 1972; 69:1583–1586. [PubMed: 4556464]
- Tronche F, Kellendonk C, Kretz O, Gass P, Anlag K, Orban PC, Bock R, Klein R, Schutz G. Disruption of the glucocorticoid receptor gene in the nervous system results in reduced anxiety. *Nat Genet.* 1999; 23:99–103. [PubMed: 10471508]
- Tucker P, Laemle L, Munson A, Kanekar S, Oliver ER, Brown N, Schlecht H, Vetter M, Glaser T. The eyeless mouse mutation (*ey1*) removes an alternative start codon from the *Rx/rax* homeobox gene. *Genesis.* 2001; 31:43–53. [PubMed: 11668677]
- Vandesompele J, De Preter K, Pattyn F, Poppe B, Van Roy N, De Paepe A, Speleman F. Accurate normalization of real-time quantitative RT-PCR data by geometric averaging of multiple internal control genes. *Genome Biol.* 2002; 3 RESEARCH0034.
- VanDunk C, Hunter LA, Gray PA. Development, maturation, and necessity of transcription factors in the mouse suprachiasmatic nucleus. *J Neurosci.* 2011; 31:6457–6467. [PubMed: 21525287]
- Wiegand SJ, Terasawa E. Discrete lesions reveal functional heterogeneity of suprachiasmatic structures in regulation of gonadotropin secretion in the female rat. *Neuroendocrinology.* 1982; 34:395–404. [PubMed: 6808412]

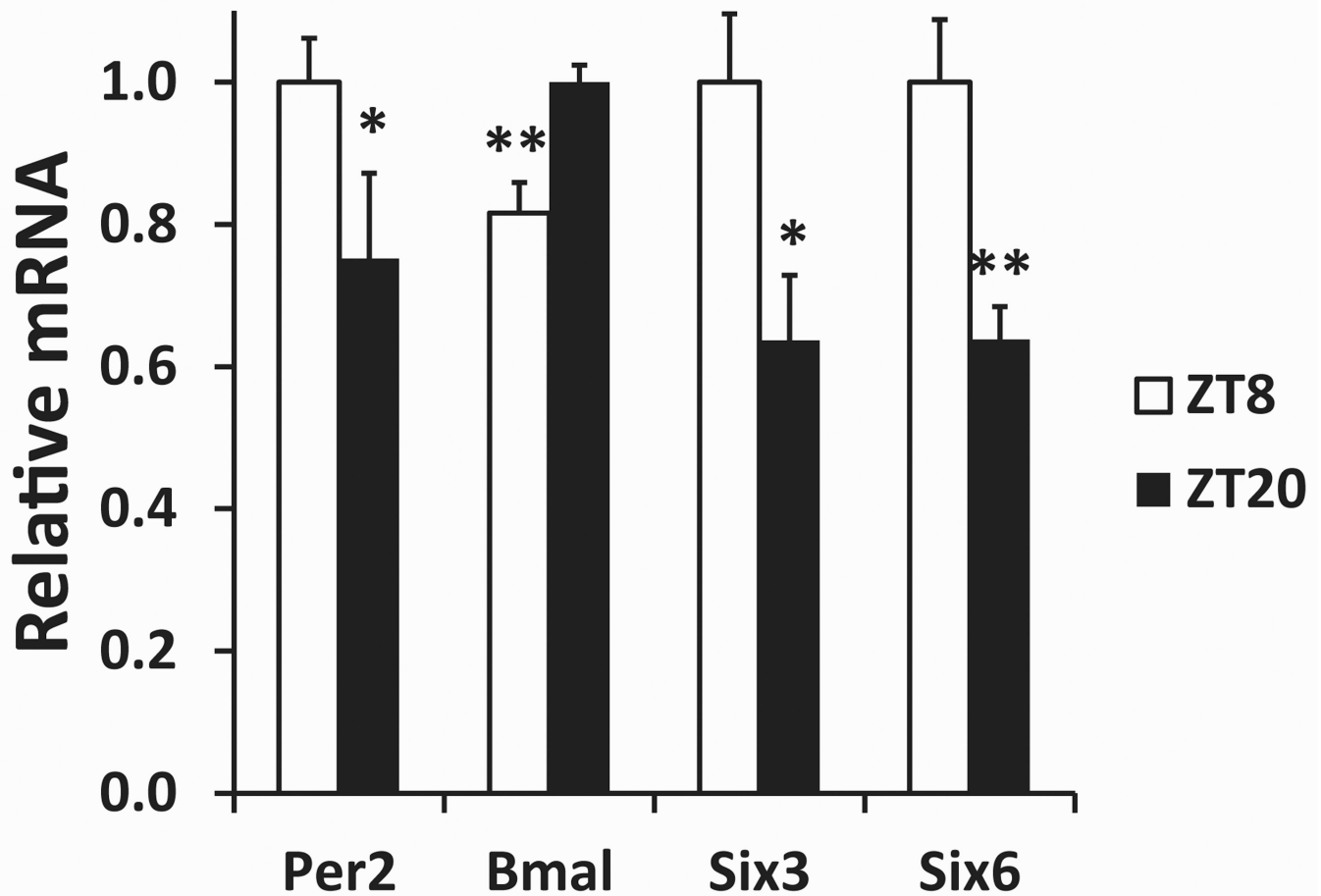


**Figure 1.**

Hypothalamic gene expression at 2 points in zeitgeber time. Gene expression data obtained via quantitative reverse-transcription PCR. Each gene's expression has been normalized to the geometric mean of 3 control genes (see the Materials and Methods section) and is expressed relative to the peak average value between the 2 groups, ZT8 ( $n = 4$ ) and ZT20 ( $n = 4$ ). \*Statistically significant difference in expression ( $p < 0.05$  via Student  $t$  test) between the ZT8 and ZT20 groups for each gene. \*\* $p < 0.01$ .

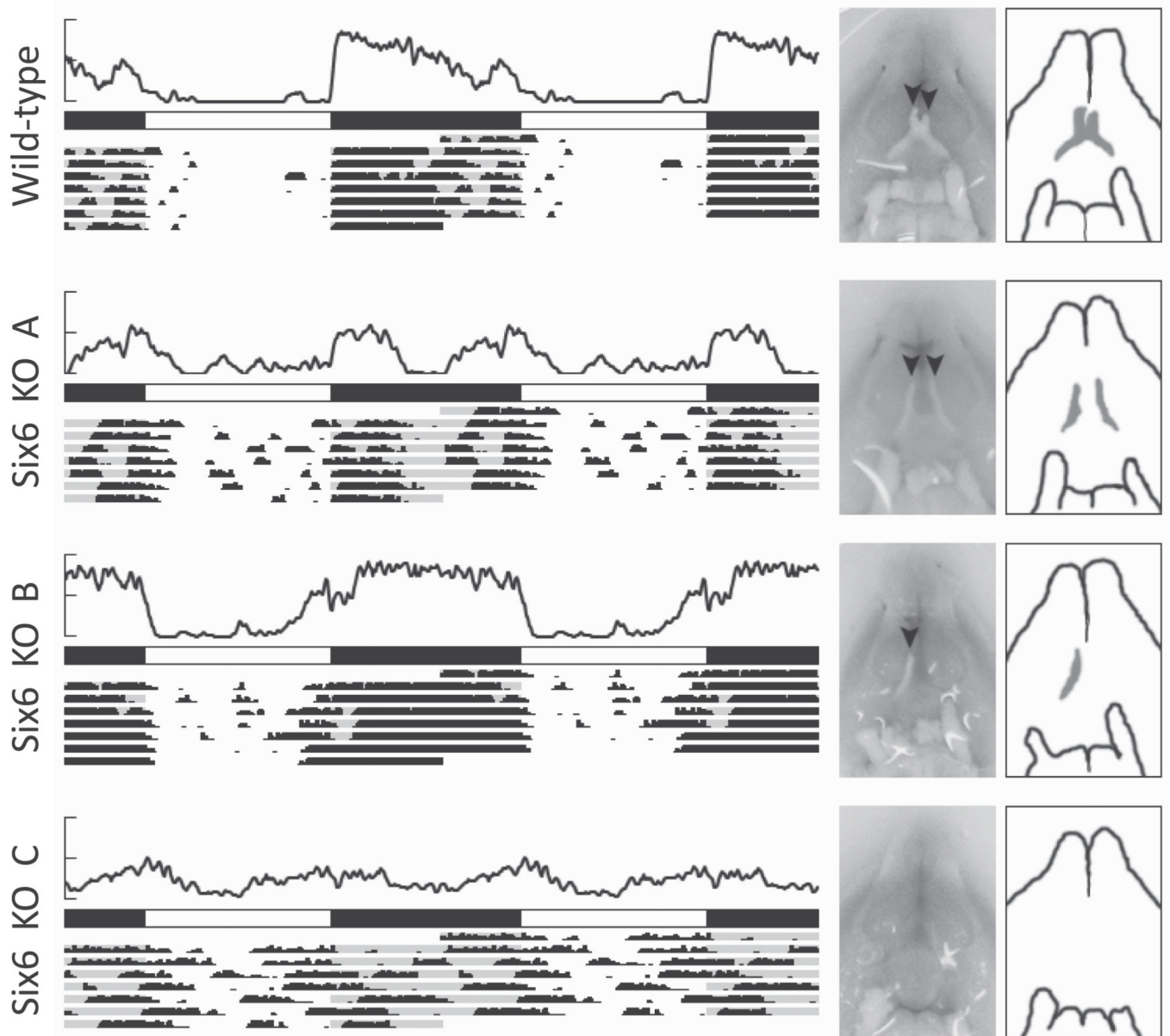


**Figure 2.**

Wheel-running activity and optic nerve phenotypes of 4 mice under L:D 12 h:12 h. For each mouse, an average activity plot (top; y-axis maximum = 500 revolutions per 6 min) is shown above photoperiod (filled = dark, open = light) and actograms representing 7 days of wheel-running data (each actogram is double-plotted such that 48 h of data are shown for each row). To the right of the activity are photographs and schematic drawings of each mouse's optic nerve phenotype. The ventral surface of each brain is shown, with the location of the optic chiasm centered. Black arrowheads represent the presence of optic nerves.

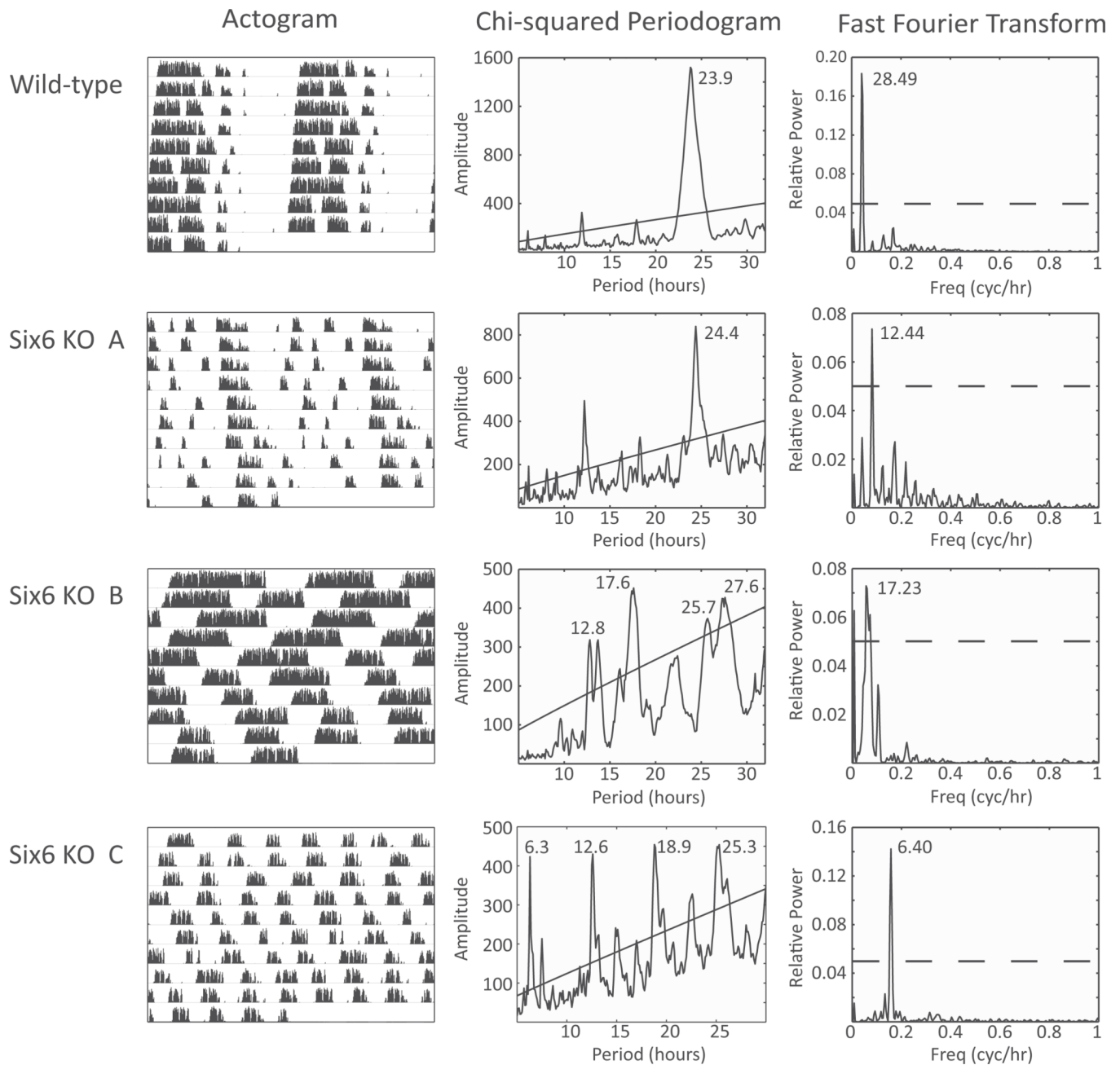


**Figure 3.** Wheel-running activity during constant darkness. (Left) Wild-type and *Six6*-null mouse wheel-running actograms are shown for 10 days of activity in constant darkness. (Middle)  $\chi^2$  periodogram analysis of the actogram data. Diagonal line represents  $p = 0.05$  significance threshold. (Right) Fast Fourier transform of the actogram data. Peak period listed; dotted line represents 0.05 relative power. Knockout mice A, B, and C are the same individual animals as in Figure 2.

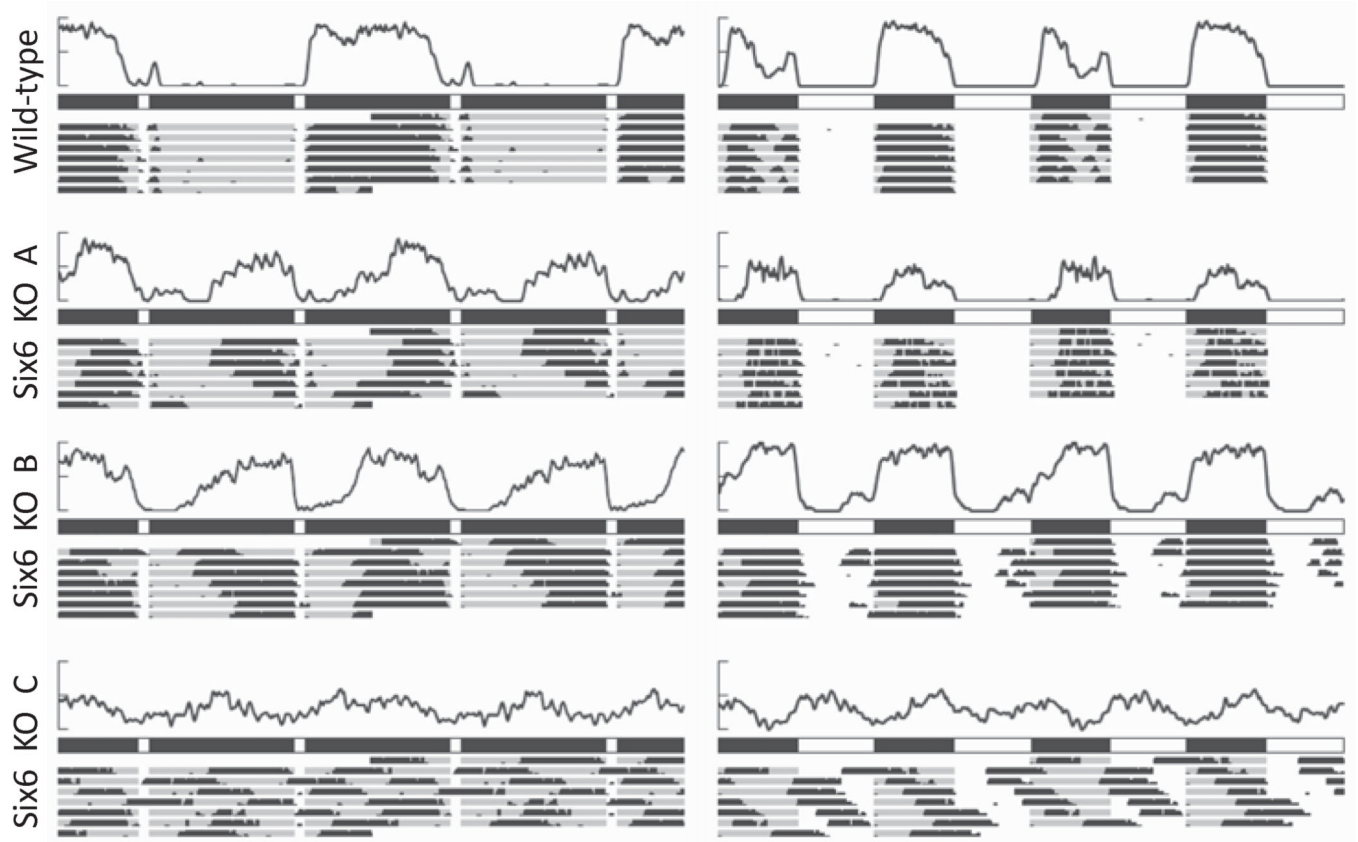


**Figure 4.**

Wheel-running activity during skeleton and bifurcation photoperiods. (Left) Wild-type and knockout mouse average activity (top) and actogram (bottom) during 7 days of activity in a skeleton photoperiod of 1 h:11 h L:D. (Right) Wild-type and knockout mouse average activity (top), photoperiod (middle), and actogram (bottom) during 7 days of activity in a bifurcated 6 h:6 h:6 h L:D:L:D photoperiod. As in Figure 2, each activity average and actogram is double-plotted over 48 h of activity. Knockout mice A, B, and C are the same individual animals as in Figures 2 and 3.

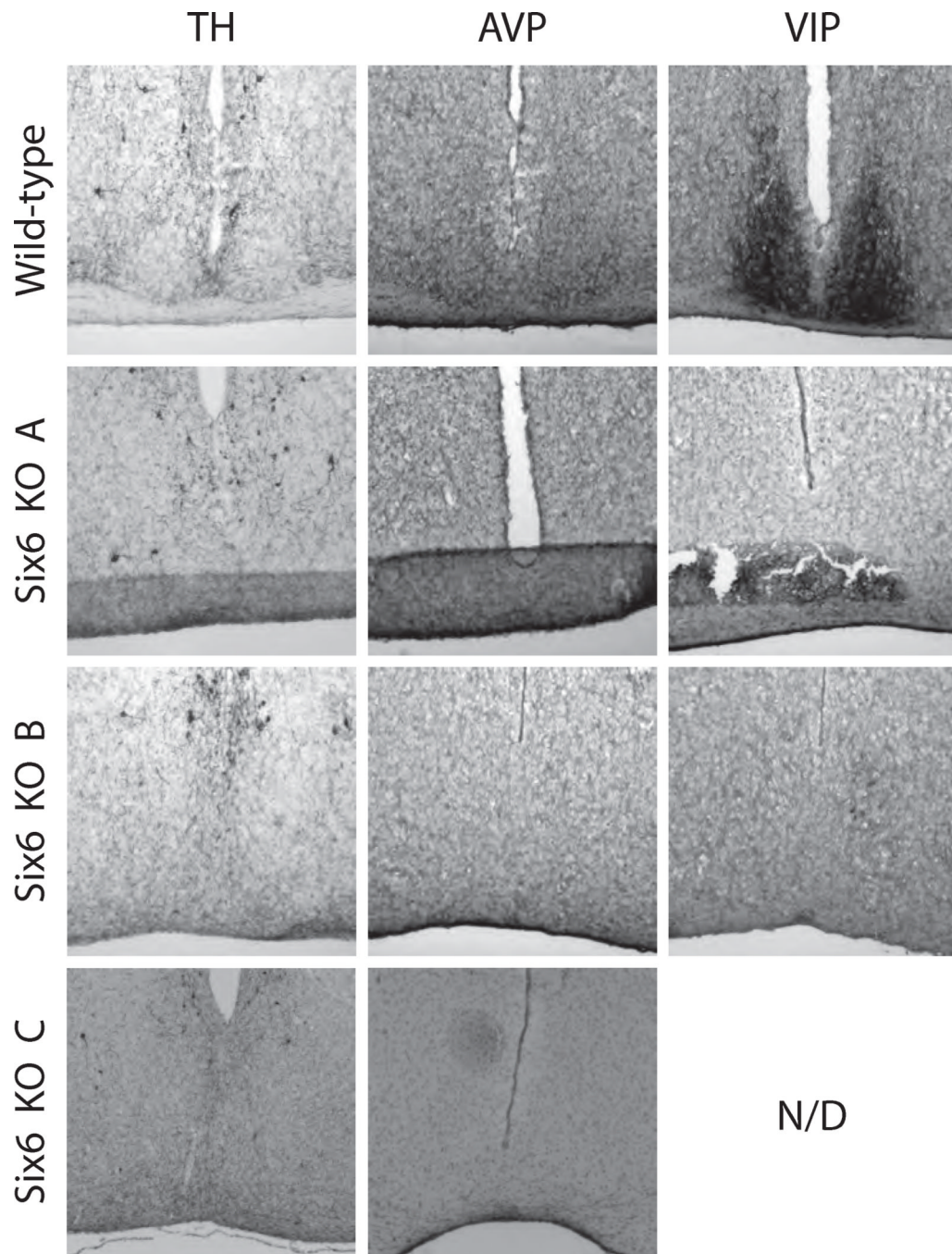


**Figure 5.** SCN of 1 wild-type (WT) and 3 *Six6*-null mice used in the behavioral tests. Tyrosine hydroxylase (TH) and arginine vasopressin (AVP), and vasoactive intestinal polypeptide (VIP) immunohistochemical staining of WT and *Six6*-null (KO) mouse hypothalami at the level of the SCN. Supplemental Figure S2 includes these data along with neighboring rostral and caudal coronal sections for all image series. Knockout mice A, B, and C are the same individual animals as in Figures 2 to 4.

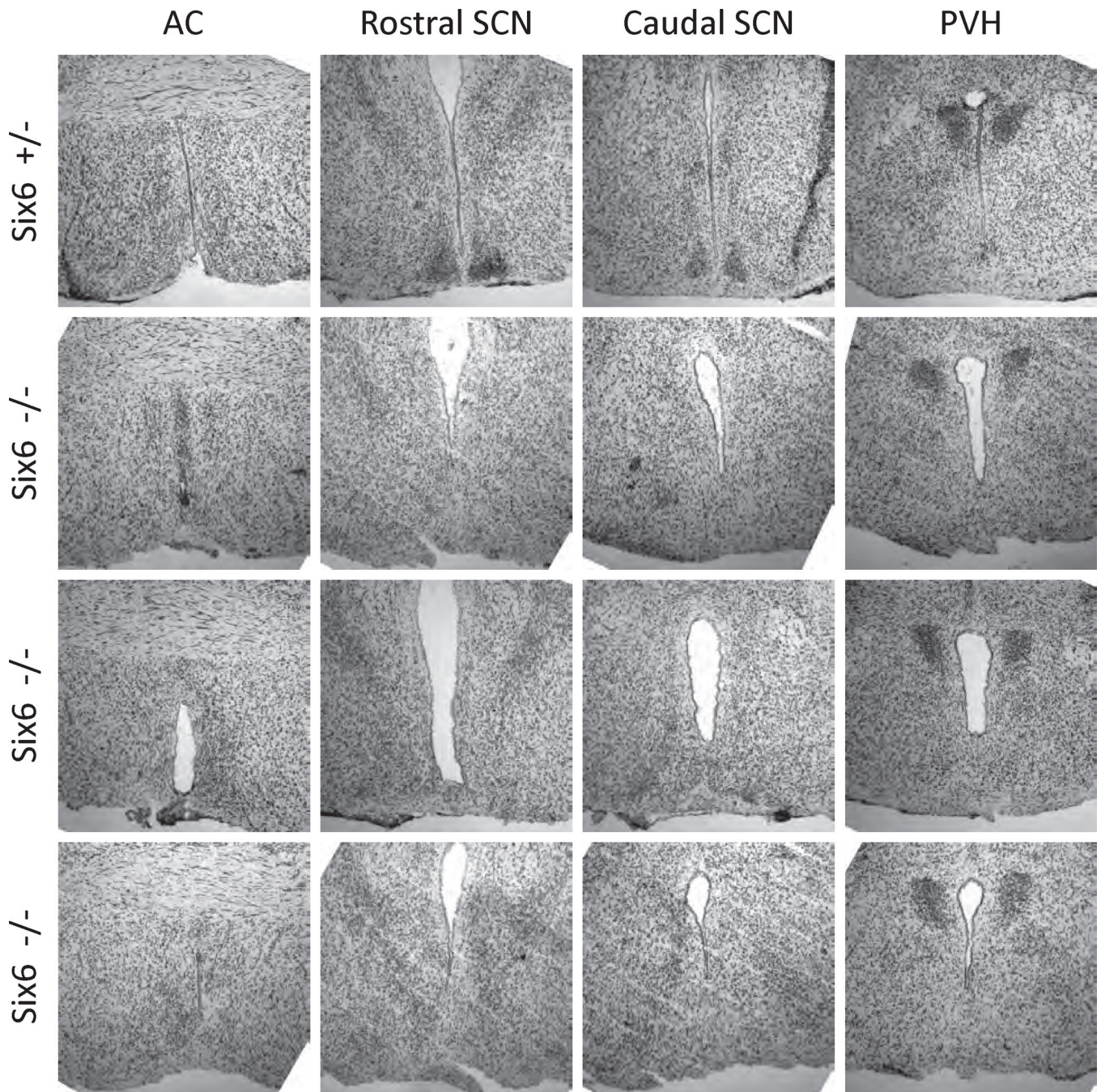
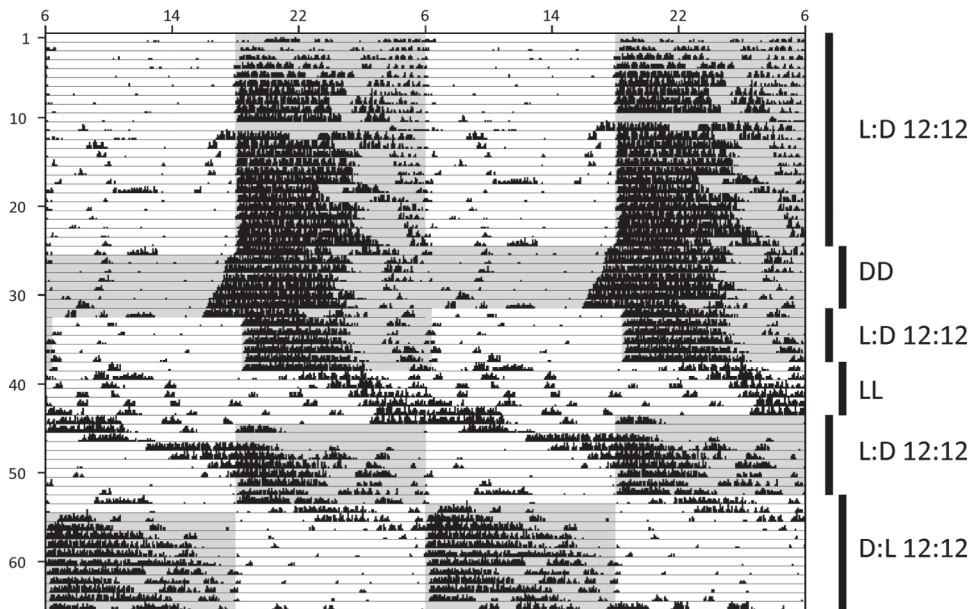


**Figure 6.**

SCN of heterozygous and *Six6*-null mice: cresyl violet Nissl staining. Mice heterozygous for the *Six6*-null allele (*Six6* +/-) display normal SCN morphology, assessed qualitatively by dense nuclei of cell bodies ( $n = 3$ , 1 shown). *Six6*-null mice ( $n = 3$ ) do not show normal SCN morphology, despite normal histology at the level of the anterior commissure (AC; leftmost column) and apparently normal paraventricular nuclei (PVH; rightmost column).

## Sham surgery on day 11



## Optic nerve crushed on day 11

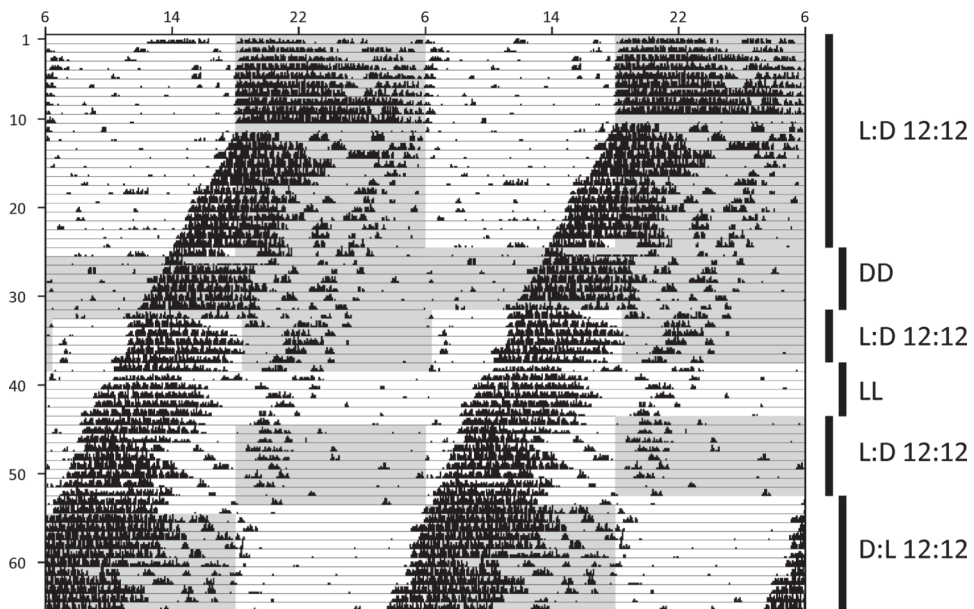


**Figure 7.** Circadian behavior following optic nerve crush. Behavioral actograms of wild-type mice receiving either sham optic nerve surgery (top) or optic nerve crush surgery (bottom) on day 11 of activity monitoring. Six different photoperiod manipulations were performed as shown (DD = constant darkness, LL = constant light), with the gray background indicating lights-off and white background indicating lights-on. Data are double-plotted across each row of the actogram (48 h total).